



# Wet-chemical dip-coating preparation of highly oriented copper–aluminum oxide thin film and its opto-electrical characterization

Arghya Banerjee<sup>a</sup>, Kalyan K. Chattopadhyay<sup>b</sup>, Sang W. Joo<sup>a,\*</sup>

<sup>a</sup> School of Mechanical Engineering, Yeungnam University, Gyongsan 712-749, South Korea

<sup>b</sup> Department of Physics, Jadavpur University, Kolkata-700032, India

## ARTICLE INFO

### Article history:

Received 10 March 2010

Received in revised form

6 August 2010

Accepted 21 October 2010

### Keywords:

CuAlO<sub>2</sub>

p-Type semiconductor

Transparent

Wet-chemical synthesis

Optical properties

Electrical properties

## ABSTRACT

Transparent p-type semiconducting copper aluminum oxide thin film has been synthesized by a wet-chemical route. CuCl and AlCl<sub>3</sub>, dissolved in HCl, are taken as starting materials. pH value of the solution is controlled by adding a measured amount of NaOH into it. Films are deposited by dip-coating technique on glass and Si substrates followed by annealing in air at 500 °C for 3 h. XRD pattern confirms the crystalline CuAlO<sub>2</sub> phase formation in the film and also indicates a strong (0 0 6) orientation. UV–vis spectrophotometric measurements show high transparency of the film in the visible region with a direct allowed bandgap of 3.94 eV. Electrical measurements depict the thermally activated conduction within the films. Thermoelectric measurements confirm the p-type nature of the films. Compositional analysis shows the presence of excess (nonstoichiometric) oxygen within the material, which is incorporated during the air-annealing of the film. According to defect equilibrium, this excess oxygen is predicted to cause the p-type conductivity of the film. This type of cost-effective solution-based technique is very useful for volume production of this kind of technologically important material for transparent electronic and other diverse applications.

© 2010 Elsevier B.V. All rights reserved.

## 1. Introduction

The semiconducting delafossite-type oxides in the chemical form of M<sup>I</sup>M<sup>III</sup>O<sub>2</sub>, where M<sup>I</sup> is a monovalent cation (e.g. Cu<sup>I</sup>, Ag<sup>I</sup>) and M<sup>III</sup> is a trivalent cation (e.g. Al<sup>III</sup>, In<sup>III</sup>, Cr<sup>III</sup>, Co<sup>III</sup>, Fe<sup>III</sup>, Ga<sup>III</sup>, etc.), have attracted renewed interest in the field of transparent conducting thin film technology after the report of p-type conductivity in the transparent thin film of CuAlO<sub>2</sub> [1]. Most of the well-known and commonly used transparent conducting oxides (TCO) such as ZnO<sub>1-x</sub>, In<sub>1-x</sub>Sn<sub>x</sub>O<sub>3</sub>, SnO<sub>2</sub>: F/Sb/Mo, Cd<sub>2</sub>SnO<sub>4</sub>, etc. are n-type materials which are widely used in flat panel displays, solar cells and in many such applications [2–5]. After the report of p-type semiconducting, transparent CuAlO<sub>2</sub> thin film, a new field in device technology has been emerged, called the 'transparent electronics' [6], where a combination of the two types of TCOs in the form of a p–n junction could lead to a 'functional' window, which would transmit visible portion of solar radiation yet generate electricity by the absorption of UV part of it. Also CuAlO<sub>2</sub> has good thermoelectric, field-emission, ozone sensing, photochemical and photocatalytic hydrogen evolution properties as well as ferromagnetic characteristics and capability of refrigeration of electronic devices

[7–16]. Also keeping an eye in the tremendous progress in nanotechnology; fabrication and characterization of nano-structured p-CuAlO<sub>2</sub> as well as other p-TCO thin films have become an important field of work, because of new and interesting properties exhibited by these nanomaterials [16–21]. Fabrication of nano-structured p-TCOs, coupled with the already existing and well-known materials of nano-structured n-TCOs, has given an added impetus in the field of "Invisible Electronics" for the fabrication of nano active devices, which can have high efficient applications in the optoelectronics device technology. Combining all these properties CuAlO<sub>2</sub> became an important material in the last few years and attracted attention of many researchers.

For the synthesis of CuAlO<sub>2</sub> thin films, various physical and chemical procedures have been employed so far, which include pulsed laser deposition (PLD) [1,22], sputtering [23–31], microwave irradiation [32], rapid thermal annealing (RTA) [33], e-beam evaporation [34], chemical vapor deposition (CVD) [35–37], solution growth [38,39], hydrothermal process [18,40,41], spray technique [42], sol–gel deposition [43,44–46], ion exchange method [47], etc. We have chosen a cost-effective wet-chemical dip-coating technique, which is one of the most popular and wide-spread techniques in the area of thin film preparation, because of its many advantages such as easier composition control, better homogeneity, low processing temperature, lower cost, easier fabrication of large area films, possibility of using high purity starting materials and having an easy coating process of large and complex shaped substrates. As far as the synthesis of wet-chemical

\* Corresponding author. Tel.: +82 53 810 1456; fax: +82 53 810 2062.

E-mail addresses: kalyan\_chattopadhyay@yahoo.com (K.K. Chattopadhyay), sjoo@ynu.ac.kr (S.W. Joo).

process of  $\text{CuAlO}_2$  by other groups are concerned, Tonooka et al. [38] reported the synthesis of phase impure copper aluminum oxide films by solution method, using metal alkoxides and nitrates as metal sources in the precursor solutions. Li et al. [39] used similar solution process to synthesize  $\text{CuAlO}_2$  thin film using copper acetate and aluminum nitrate as metal sources. Ohashi et al. [43] used organo-metallic compounds to fabricate both phase pure and phase impure copper aluminum oxides via sol–gel process at different Cu/Al ratios. Phase pure  $\text{CuAlO}_2$  shows low mobility, which is assumed to be due to the incorporation of excessive Cu vacancies leading to the generation of strain and dislocation. Similarly, Götzendörfer et al. [44] fabricated phase pure  $\text{CuAlO}_2$  thin films via sol–gel process by using Cu-acetate and alumatrane  $[\text{Al}(\text{OCH}_2\text{CH}_2)_3\text{N}]_x$  as the metal sources. They have used a two-step thermal treatment of the as-synthesized films to get phase pure material. Few other groups [45,46] also reported the sol–gel synthesis of  $\text{CuAlO}_2$  ceramics using inorganic salts and (or) metal-organic compounds as metal sources. As far as chemical/solution syntheses of various other delafossite materials are concerned, Götzendörfer et al. [44,48] fabricated undoped and Al-doped  $\text{CuCrO}_2$  thin films via sol–gel process, Wu et al. [49] synthesized  $\text{CuFeO}_2$  powder by the sol–gel method, Beekman et al. [50] prepared  $\text{CuCoO}_2$  via ion exchange method, Okuda et al. [51] synthesized  $\text{CuCr}_{1-x}\text{Mg}_x\text{O}_2$  crystals via standard solid-state reaction, Tsuboi et al. [52] synthesized  $\text{CuYO}_2$  films via solution growth technique, Zhao et al. [53] reported the synthesis of  $\text{CuAlO}_2$  nanofibrous mats via electro-spinning process.

In our previous work [21] we have synthesized phase pure  $\text{CuAlO}_2$  nanopowders by sol–gel technique using metal nitrates and citric acid dissolved in methanol solution. Also we have reported a novel low-temperature wet-chemical synthesis route of phase pure highly crystalline  $\text{CuAlO}_2$  powders using metal oxides dissolved in molten NaOH solution at  $360^\circ\text{C}$  [54]. In this paper we have reported the fabrication of transparent conducting copper aluminum oxide thin films via wet-chemical dip-coating technique using metal chlorides as source materials dissolved in HCl followed by air-annealing at  $500^\circ\text{C}$ .

## 2. Experimental

Synthesis of copper aluminum oxide thin films on glass and Si substrates are performed in two stages. In the first stage, a sol is prepared by using HCl, cuprous chloride ( $\text{CuCl}$ , 99.99%, Loba, India) and aluminum chloride ( $\text{AlCl}_3$ , 99.99%, Merk) as metal sources. Firstly, concentrated HCl is added slowly to cuprous chloride and the solution is stirred by magnetic stirrer. During the stirring process, further addition of HCl to the solution is done until all the salts are dissolved into it. Thereafter, another solution is prepared by adding distilled water drop by drop to aluminum chloride to dissolve it completely. Then the two solutions are mixed and some excess distilled water is added to it. The mixed solution is then stirred with an elevated temperature of  $85^\circ\text{C}$  for 2 h. During the stirring process, some amount of NaOH pellets (99.99%, Loba) is added to the solution to control the pH value around 2. The solution was then aged for 3 h to get the required sol which is used for dip coating process in the second stage. Before dip coating, the glass substrates are cleaned by mild soap solution, then washed thoroughly in deionized water and also in boiling water. Finally they are ultrasonically cleaned in acetone for 15 min. For cleaning Si substrates, 20% HF solution is used and the substrates are immersed into it for 5 min to remove the native surface oxide layer. Thereafter, they are cleaned in deionized water and then with alcohol in an ultrasonic cleaner.

During dip-coating process, substrates are dipped into and then withdrawn vertically from the solution slowly at the rate of 6 cm/min for 8–10 times. Between two successive dipping, the substrate along with the sol is dried at  $100$ – $120^\circ\text{C}$  to have quick gelation. After the

dipping and withdrawing procedure, the resulting films are annealed at  $500^\circ\text{C}$  in air for 3 h to form the required  $\text{CuAlO}_2$  films.

## 3. Results and discussion

The phase identification of the sample has been carried out by room temperature X-ray diffraction (XRD, BRUKER D8 ADVANCE) using  $\text{CuK}\alpha$  radiation of wavelength  $1.5406\text{Å}$  in the  $2\theta$  range of  $20$ – $100^\circ$ . Fig. 1(a) shows the XRD pattern on Si substrate. The pattern shows a strong (0 0 6) orientation along with small peaks of (0 1 2), (1 0 7), (0 0  $\bar{1}$  2) and (1 1 6) reflections. Intensities of the smaller peaks are much less (2–7%) than that of the (0 0 6) peak, which depicts a preferential (0 0 6) orientation of our film having tetragonal crystal structure of  $\text{CuAlO}_2$  with R3m space group [55]. As shown in our XRD pattern, a small peak of  $\text{CuAl}_2\text{O}_4$  phase has been observed [56], but its intensity is much lesser (as low as 7%) than the (0 0 6) peak of  $\text{CuAlO}_2$  phase. Therefore, it may be concluded that our dip-coated copper aluminum oxide thin film has very high percentage of  $\text{CuAlO}_2$  phase with a preferred (0 0 6) orientation. Also no peaks of starting materials (e.g.  $\text{CuCl}$  and  $\text{AlCl}_3$ ) or any reactant species such as NaCl or metal oxides have been found in the pattern, which conclusively indicate that the reactants were completely mixed to form the new phase of  $\text{CuAlO}_2$ .

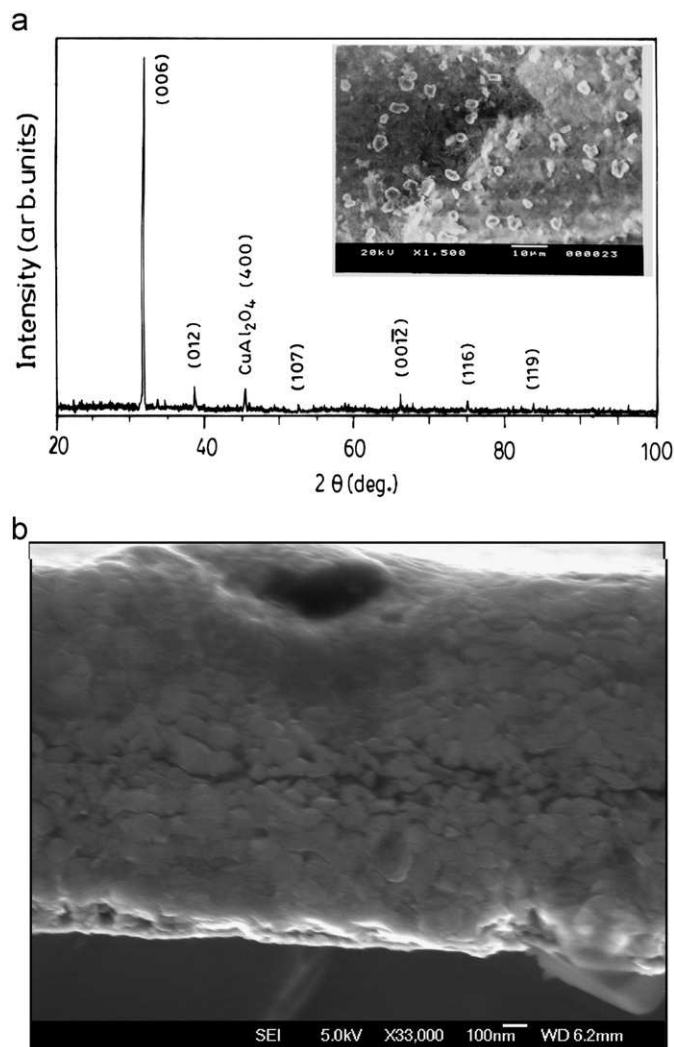


Fig. 1. (a) XRD pattern of copper aluminum oxide thin film deposited on Si substrate by wet-chemical dip-coating process. Inset: SEM micrograph of copper aluminum oxide thin film. (b) Cross-sectional SEM image of the  $\text{CuAlO}_2$  thin film.

It appears from the Cu–Al–O phase diagram [57] that  $\text{CuAlO}_2$  phase is more stable in lower temperature. At higher temperature ( $> 900^\circ\text{C}$ ),  $\text{CuAlO}_2$  can be decomposed into  $\text{CuAl}_2\text{O}_4$  and  $\text{CuO}$  according to the following reaction [39]:



This kind of behavior is observed by Lan et al. [58] where they found the similar decomposition of sputter-deposited  $\text{CuAlO}_2$  thin film into  $\text{CuAl}_2\text{O}_4$  and  $\text{CuO}$  when annealed around  $900^\circ\text{C}$ . Unlike other groups, who have started with Cu(II) state [39,42,44–46] in the precursor materials, we have started with Cu(I) salt ( $\text{CuCl}$ ), and, hence it is expected that greater percentage of +1 state of copper will be present in both the precursor as well as in the initial film. During air-annealing process a small fraction of Cu(I) state might have been converted to Cu(II) state to form the spinel phase according to Eq. (1). But as the annealing temperature is considerably low, a large fraction of the film phase will remain in delafossite state and only a very small amount will be converted into spinel phase. That is why we have obtained a mixed phase of  $\text{CuAlO}_2$  and  $\text{CuAl}_2\text{O}_4$  in our film with the later phase only less than 7% of the delafossite one (cf. Fig. 1a). This may be the reason for a large fraction of the copper to maintain its +1 state even without using elevated and controlled annealing atmosphere, whereas other groups used high temperature multi-step thermal treatments [44] of the films to get phase pure material. Our aim is to get an optimum annealing temperature in ambient atmosphere to get high percentage of delafossite phase and we have achieved that for an annealing temperature around  $500^\circ\text{C}$ .

Surface morphology of the as-synthesized film is studied with Scanning Electron Microscopic imaging (SEM, JEOL-5200). Inset of Fig. 1(a) shows the scanning electron micrograph of a typical  $\text{CuAlO}_2$  thin film deposited on glass substrate. Existence of a smooth surface with finer grains and well defined grain boundaries are observed. Some bigger clusters are also shown to be dispersed on the surface, which resulted due to the agglomeration of finer grains. Cross-sectional SEM image has been shown in Fig. 1(b). The micrograph reveals the thickness of the film around  $1.5\ \mu\text{m}$ . Dense granular structures are observed in the image with some voids are visible at the middle of the structure. From the image it appears that the voids create a separation layer between the upper and lower parts of the film cross-section. These layers can be attributed to the multi-step coating procedure adopted to deposit the film via dip-coating process. Similar type of multilayer structure has been reported by Götzendörfer et al. [44] for their sol–gel dip-coated  $\text{CuAlO}_2$  thin film, and they attributed this phenomenon to the different crystallization energetics present for different layers of the film. In our case also similar phenomenon may be responsible for the layered structure shown in the micrograph. But it is also to be noted that from the image it appears that both the layers are having similar types of crystallinity. Therefore, we assume that due to low annealing temperature, the densification of the film has not taken place fully and a further elevated thermal treatment may reduce these voids. But in that scenario, there will always be a high probability of decomposition of the film to spinel phase, as discussed earlier. So there will be a trade-off between the proper phase formation and densification of the film, which is the further course of our research to study the structural properties of the film with respect to various annealing temperatures.

Optical characterizations of the films deposited on glass substrates have been performed by measuring transmittance in the wavelength region 300–800 nm using a UV–vis spectrophotometer (HITACHI-U-3410). Fig. 2 shows the transmittance spectrum of  $\text{CuAlO}_2$  thin film deposited on glass substrate, taking similar glass as reference. Hence the spectrum is solely for the films. It shows almost 80–90% transmittance in the visible region. With the known film thickness as measured from the cross-sectional SEM,

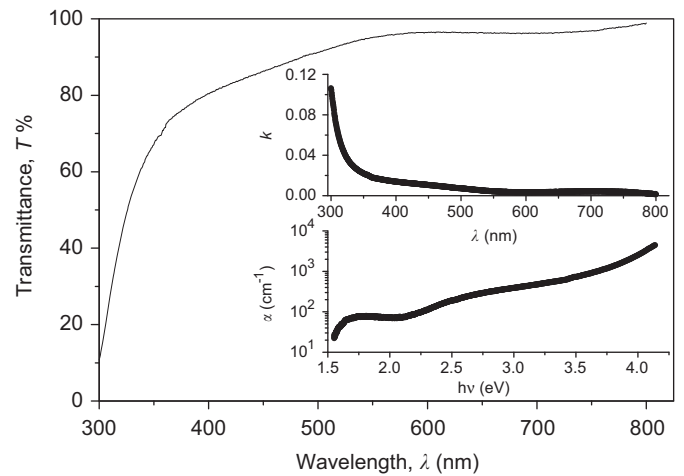


Fig. 2. Optical transmittance ( $T$ ) spectra of wet-chemical dip-coated copper aluminum oxide thin film deposited on glass substrate. Inset: Spectral variations of absorption coefficient ( $\alpha$ ) and extinction coefficient ( $k$ ) of the copper aluminum oxide thin film. The calculations for  $\alpha$  and  $k$  are done from the transmittance data.

absorption coefficients ( $\alpha$ ) are calculated from the transmittance data using the Manifacier model [59] as

$$\alpha = \frac{1}{d} \ln\left(\frac{1}{T}\right) \quad (2)$$

where  $d$  is the film thickness and  $T$  is the transmittance of the film (here we have neglected the reflectance of the film which would be very small for transparent films).

Also the extinction coefficients ( $k$ ) are calculated from the values of  $\alpha$  calculated from Eq. (1) over the measured wavelength ( $\lambda$ ) range according to the formula:

$$k = \frac{\lambda\alpha}{4\pi} \quad (3)$$

Spectral variations of the extinction coefficients ( $k$ ) and absorption coefficients ( $\alpha$ ) over the measured wavelength range are shown in the insets of Fig. 2. The values of  $k$  vary from  $1.42 \times 10^{-3}$  to  $10.62 \times 10^{-2}$ , whereas the values of  $\alpha$  vary from  $22.0$  to  $4.5 \times 10^2\ \text{cm}^{-1}$  in the wavelength range of 300–800 nm. These values are comparable to the sputtered  $\text{CuAlO}_2$  films reported by us previously [28,29]. The fundamental absorption, which corresponds to electron excitation from the valance band to conduction band, can be used to determine the nature and value of the optical bandgap. The relation between the absorption coefficients ( $\alpha$ ) and the incident photon energy ( $h\nu$ ) can be written as [60]

$$(\alpha h\nu)^{1/n} = A(h\nu - E_g) \quad (4)$$

where  $A$  is a constant and  $E_g$  is the bandgap of the material and exponent  $n$  depends on the type of transition. For direct allowed transition,  $n=1/2$ , indirect allowed transition,  $n=2$  and for direct forbidden transition,  $n=3/2$ . To determine the possible transitions,  $(\alpha h\nu)^{1/n}$  vs.  $h\nu$  are plotted for different values of  $n$ . The  $(\alpha h\nu)^2$  vs.  $h\nu$  and  $(\alpha h\nu)^{1/2}$  vs.  $h\nu$  plots are shown in Fig. 3 and the inset, respectively. Extrapolating the linear portions of the graphs to the  $h\nu$  axes, we have obtained the direct and indirect band gaps from the intercept on  $h\nu$  axes which come out to be 3.94 and 2.42 eV, respectively. These values agree well with the values reported previously [1,22,28,29].

Electrical characterizations (mainly the sheet resistance and temperature dependence of conductivity) of the copper aluminum oxide thin film have been performed by linear four-probe method using Keithley multimeter (Model 6514). The contact was made with silver paint, which showed linear  $I$ – $V$  characteristic over a wide range of applied voltage. Fig. 4 represents  $\ln\sigma$  vs.  $1/T$  plot of the  $\text{CuAlO}_2$  film on glass substrate from room temperature (300 K)

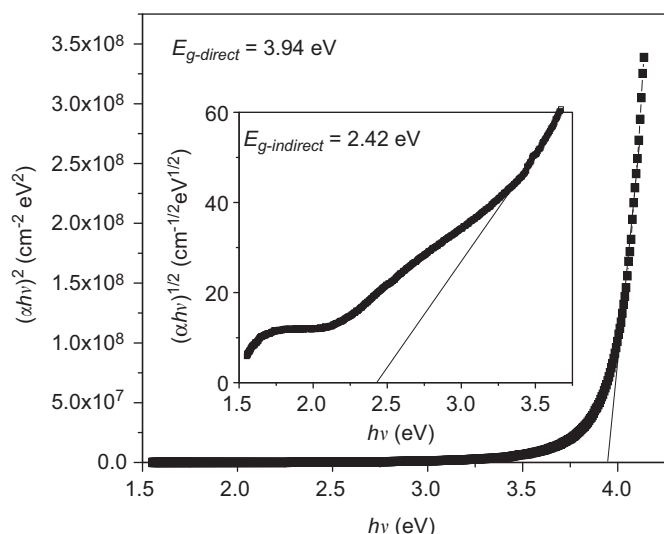


**Fig. 3.** Calculations of the optical bandgap (direct bandgap,  $E_{g-direct}$ ) of copper aluminum oxide thin film. Inset: Determination of indirect ( $E_{g-indirect}$ ) bandgap.

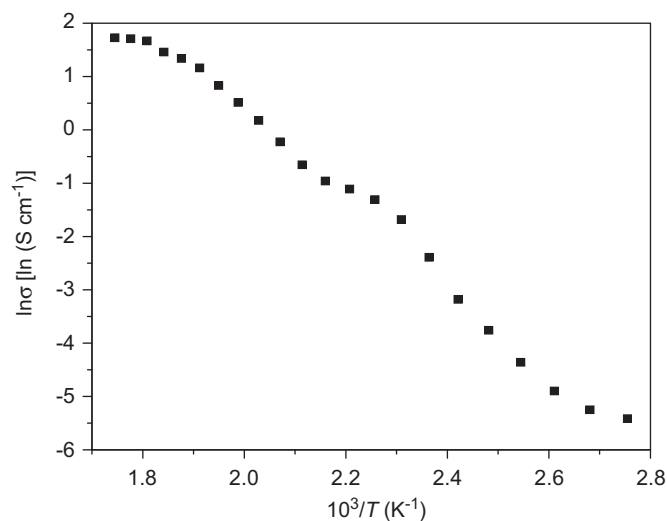


**Fig. 4.** Temperature variation of the conductivity of wet-chemical dip-coated copper aluminum oxide thin film on glass substrate.

to 575 K. The straight-line nature of the Arrhenius plot indicates the thermally activated conduction, as often found in semiconductors. Room temperature conductivity ( $\sigma_{RT}$ ) of the film is obtained as  $0.004 \text{ S cm}^{-1}$ . This value is comparable to the previously reported copper aluminum oxide films prepared by chemical routes by Tonooka ( $0.005 \text{ S cm}^{-1}$ ), Bouzidi ( $0.004 \text{ S cm}^{-1}$ ) and co-authors [38,42]. But, this value of  $\sigma_{RT}$  for our chemically deposited film is one to two orders of magnitude less than that of  $\text{CuAlO}_2$  films prepared by physical techniques [8,10,11,22]. This is mainly due to the higher number of defect states formed within the film, which is generally observed for films synthesized by wet-chemical techniques. Also from the slope of the graph we get the value of activation energy ( $E_a$ ) which corresponds to the minimum energy required to transfer carriers from acceptor level to the valence band (for p-type materials) and the value of  $E_a$  comes out as 740 meV. This value is higher than that obtained by others and us [1,28] as expected for our comparatively high resistive film.

p-Type nature of the as-synthesized copper aluminum oxide thin film is confirmed by both hot-probe method and thermoelectric measurements. Thermopower measurements are performed over

the temperature range 300–500 K. For thermoelectric power measurement (temperature variation of Seebeck coefficient), a temperature gradient across the sample was created by keeping one end of the film in a hot head and the other in a cold head. The hot-head temperature was varied from room temperature to 500 K, whereas the cold head was kept at room temperature. And these temperatures of the hot and cold-ends of the film were measured by proper thermocouple arrangements. The thermo-emfs generated between the hot and cold-ends of the sample, at different hot end temperatures, were used to determine the Seebeck coefficients ( $S$ ) of the material. The entire system was kept under vacuum condition. Positive values of the Seebeck coefficients indicate p-type nature of the films with room temperature Seebeck coefficient ( $S_{RT}$ ) is obtained around  $+206 \mu\text{V K}^{-1}$ . This value is higher than the sputter-deposited  $\text{CuAlO}_2$  thin films ( $\sim 120 \mu\text{V K}^{-1}$ ) reported by us previously [28,29]. In general, for simple materials, a decrease in  $\sigma$  leads to an increase in  $S$ . For our sol-gel deposited films, the conductivity is lower than the sputter-deposited films, which leads to an increase in the  $S$  values.

It is well-known that the p-type nature of copper aluminum oxide is due to the intercalation of nonstoichiometric (excess) oxygen within the material. The chemical formula of this material is considered as  $\text{CuAlO}_{2+x}$ , with the value of  $x$  ranging from as low as  $2 \times 10^{-5}$  [1] to as high as 0.24 [49] over the stoichiometric value. The approximate defect equilibrium can be represented as [61–63]



where  $\text{O}_\text{O}$ ,  $\text{V}_\text{Cu}$ ,  $\text{V}_\text{Al}$  and  $h$  denote lattice oxygen, Cu vacancy, Al vacancy and hole, respectively. Superscripts  $\times$ ,  $-$  and  $+$  denote effective neutral, negative and positive charge states, respectively. As mentioned earlier, we have annealed our sample in air for 3 h to get the proper phase of the materials. This annealing procedure has also facilitated the excess oxygen intercalation within the material that provides the p-type conductivity of the film. To determine the presence of excess oxygen within the thin film, we have performed the compositional analyses of the film by energy dispersive X-ray analysis (EDX, Leica S-440, Oxford ISIS), which could detect elements from boron (5) to uranium (92). The atomic % of excess oxygen is determined to be around 0.25, which leads to a chemical formula of  $\text{CuAlO}_{2+0.005}$ . But this formula may not be logical as there is a small amount of  $\text{CuAl}_2\text{O}_4$  present within the film (as shown in the XRD analysis in Fig. 1a), which modifies the EDX results. Also the electrical conductivity is much lesser than that expected with the amount of excess oxygen present within the sample [61]. This is mainly because our sol-gel deposited copper aluminum oxide thin film contains non-delafossite phase as well as some defect states that modify the conductivity, which is common for solution-deposited thin films [38,42,44]. Synthesis of phase pure, high conducting film is the further course of our research work.

#### 4. Conclusions

Wet-chemical synthesis of transparent copper aluminum oxide thin films has been performed successfully. XRD pattern confirms the proper phase formation of the film with a strong (0 0 6) orientation. Optical transmittance spectrum depicts almost 90% transparency of the film in the wavelength range of 500–800 nm, with a direct allowed bandgap of 3.94 eV. Electrical characterization shows room-temperature conductivity around  $4.0 \times 10^{-3} \text{ S cm}^{-1}$ . This value is relatively lower than previously reported  $\text{CuAlO}_2$  film deposited by physical techniques but comparable to the solution-based processes reported earlier. Generally, wet-chemical technique produces films with higher resistivity mainly because of the presence of various other species within the film (as well as some defect states at grain boundaries) generated during aqueous chemical process. Hot-probe

and thermoelectric measurements confirm the p-type nature of the film. Compositional analysis confirms the presence of excess oxygen within the film. This excess oxygen, incorporated by air-annealing during deposition, is supposed to be responsible for the p-type nature of the film. The cost-effective, simple, solution-based method to deposit this type of technologically important materials is very important in potential volume production for diverse device applications.

## Acknowledgement

This work is supported by the World Class University Grant no. R32-2008-000-20082-0 of the Ministry of Education, Science and Technology of Korea.

## References

- [1] H. Kawazoe, M. Yasukawa, H. Hyodo, M. Kurita, H. Yanagi, H. Hosono, *Nature* 389 (1997) 939.
- [2] I. Hamberg, C.G. Granqvist, *J. Appl. Phys.* 60 (1986) R123.
- [3] K.L. Chopra, S. Major, D.K. Pandya, *Thin Solid Films* 102 (1983) 1.
- [4] H. Cachet, A. Gamard, G. Campet, B. Jousseume, T. Toupance, *Thin Solid Films* 388 (2001) 41.
- [5] R. Wendt, K. Ellmer, *Surf. Coat. Technol.* 93 (1997) 27.
- [6] G. Thomas, *Nature* 389 (1997) 907.
- [7] K. Koumoto, H. Koduka, W.S. Seo, *J. Mater. Chem.* 11 (2001) 251.
- [8] A.N. Banerjee, R. Maity, P.K. Ghosh, K.K. Chattopadhyay, *Thin Solid Films* 474 (2005) 261.
- [9] K. Park, K.Y. Ko, W.-S. Seo, *Mater. Sci. Eng. B* 129 (2006) 1.
- [10] A.N. Banerjee, K.K. Chattopadhyay, *Appl. Surf. Sci.* 225 (2004) 213.
- [11] A.N. Banerjee, C.K. Ghosh, S. Das, K.K. Chattopadhyay, *Physica B* 370 (2005) 264.
- [12] X.G. Zheng, K. Taniguchi, A. Takahashi, Y. Liu, C.N. Xu, *Appl. Phys. Lett.* 85 (2004) 1728.
- [13] R. Brahimi, M. Trari, A. Bouguelia, Y. Bessekhouad, *J. Solid, State Electrochem.* doi:10.1007/s10008-009-0935-x.
- [14] N. Koriche, A. Bouguelia, A. Aider, M. Trari, *Int. J. Hydrogen Energy* 30 (2005) 693.
- [15] H. Kizaki, K. Sato, A. Yanase, H. Katayama-Yoshida, *Physica B* 376–377 (2006) 812.
- [16] K. Park, K.Y. Ko, W.-S. Seo, *J. Eur. Ceram. Soc.* 25 (2005) 2219.
- [17] H. Gong, Y. Wang, Y. Luo, *Appl. Phys. Lett.* 76 (2000) 3959.
- [18] S. Gao, Y. Zhao, P. Gou, N. Chen, Y. Xie, *Nanotechnology* 14 (2003) 538.
- [19] A.N. Banerjee, K.K. Chattopadhyay, *J. Appl. Phys.* 97 (2005) 084308.
- [20] T. Prakash, K.P. Prasad, S. Ramasamy, B.S. Murty, *J. Nanosci. Nanotechnol.* 8 (2008) 4273.
- [21] C.K. Ghosh, S.R. Popuri, T.U. Mahesh, K.K. Chattopadhyay, *J. Sol–Gel Sci. Technol.* 52 (2009) 75.
- [22] H. Yanagi, H. Kawazoe, A. Kudo, M. Yasukawa, H. Hosono, *J. Electroceram.* 4 (2000) 427.
- [23] R.E. Stauber, J.D. Perkins, D.S. Perkins, *Electrochem. Solid-State Lett.* 2 (1999) 654.
- [24] A.N. Banerjee, S. Nandy, C.K. Ghosh, K.K. Chattopadhyay, *Thin Solid Films* 515 (2007) 7324.
- [25] C.H. Ong, H. Gong, *Thin Solid Films* 445 (2003) 299.
- [26] N. Tsuboi, Y. Takahashi, S. Kobayashi, H. Shimizu, K. Kato, F. Kaneko, *J. Phys. Chem. Solids* 64 (2003) 1671.
- [27] E.M. Alkoy, P. Kelly, *J. Vacuum* 75 (2005) 221.
- [28] A.N. Banerjee, S. Kundoo, K.K. Chattopadhyay, *Thin Solid Films* 440 (2003) 5.
- [29] A.N. Banerjee, R. Maity, K.K. Chattopadhyay, *Mater. Lett.* 58 (2003) 10.
- [30] G. Dong, M. Zhang, W. Lan, P. Dong, H. Yan, *Vacuum* 82 (2008) 1321.
- [31] G.B. Dong, M. Zhang, W. Lan, P.M. Dong, X.P. Zhao, H. Yan, *J. Mater. Sci.: Mater. Electron.* 20 (2009) 193.
- [32] L. Torkian, M.M. Amini, *Mater. Lett.* 63 (2009) 587.
- [33] J.H. Shy, B.H. Tseng, *J. Phys. Chem. Solids* 66 (2005) 2123.
- [34] D.-S. Kim, S.-Y. Choi, *Phys. Status Solidi (A)* 202 (2005) R167.
- [35] Y. Wang, H. Gong, *Adv. Mater. CVD* 6 (2000) 285.
- [36] H. Gong, Y. Wang, Y. Luo, *Appl. Phys. Lett.* 76 (2000) 3959.
- [37] Y. Wang, H. Gong, F. Zhu, L. Liu, L. Huang, A.C.H. Huan, *Mater. Sci. Eng. B* 85 (2001) 131.
- [38] K. Tonoooka, K. Shimokawa, O. Nishimura, *Thin Solid Films* 411 (2002) 129.
- [39] G. Li, X. Zhu, H. Lei, H. Jiang, W. Song, Z. Yang, J. Dai, Y. Sun, X. Pan, S. Dai, *J. Sol–Gel Sci. Technol.* 53 (2010) 641.
- [40] D.Y. Shahriari, A. Barnabè, T.O. Mason, K.R. Poeppelmeier, *Inorg. Chem.* 40 (2001) 5734.
- [41] T. Sato, K. Sue, H. Tsumatori, M. Suzuki, S. Tanaka, A. Kawai-Nakamura, K. Saitoh, K. Aida, T. Hiaki, *J. Supercritical Fluids* 46 (2008) 173.
- [42] C. Bouzidi, H. Bouzouita, A. Timoumi, B. Rezig, *Mater. Sci. Eng. B* 118 (2005) 259.
- [43] M. Ohashi, Y. Iida, H. Morikawa, *J. Am. Ceram. Soc.* 85 (2002) 270.
- [44] S. Götzendörfer, C. Polenzky, S. Ulrich, P. Löbmann, *Thin Solid Films* 518 (2009) 1153.
- [45] J. Ding, Y. Sui, W. Fu, H. Yang, S. Liu, Y. Zeng, W. Zhao, P. Sun, J. Guo, H. Chen, M. Li, *Appl. Surf. Sci.* 256 (2010) 6441.
- [46] Z. Deng, X. Zhu, R. Tao, W. Dong, X. Fang, *Mater. Lett.* 61 (2007) 686.
- [47] L. Dloczik, Y. Tomm, R. Könenkamp, *Thin Solid Films* 451–452 (2004) 116.
- [48] S. Götzendörfer, R. Bywalez, P. Löbmann, *J. Sol–Gel Sci. Technol.* 52 (2009) 113.
- [49] R. Wu, W. Pen, S. Liu, J. Li, *Key Eng. Mater.* 368–372 (2009) 663.
- [50] M. Beekman, J. Salvador, X. Shi, G.S. Nolas, J. Yang, *J. Alloys Compd.* 489 (2010) 336.
- [51] T. Okuda, Y. Beppu, Y. Fujii, T. Onoe, N. Terada, S. Miyasaka, *Phys. Rev. B* 77 (2008) 134423.
- [52] N. Tsuboi, K. Tosaka, S. Kobayashi, K. Kato, F. Kaneko, *Jpn. J. Appl. Phys.* 47 (2008) 588.
- [53] S. Zhao, M. Li, X. Liu, G. Han, *Mater. Chem. Phys.* 116 (2009) 615.
- [54] B. Saha, R. Thapa, K.K. Chattopadhyay, *Mater. Lett.* 63 (2009) 394.
- [55] J.C.P.D.S. Powder Diffraction File Card #09-185.
- [56] J.C.P.D.S. Powder Diffraction File Card #35-1401.
- [57] B.J. Ingram, T.O. Mason, R. Asahi, K.T. Park, A.J. Freeman, *Phys. Rev. B* 64 (2001) 155114.
- [58] W. Lan, M. Zhang, G.B. Dong, Y.Y. Wang, H. Yan, *J. Mater. Res.* 22 (2007) 3338.
- [59] J.C. Manificier, J. Gasiot, J.P. Fillard, *J. Phys. E* 9 (1976) 1002.
- [60] J.I. Pankove, *Optical Processes in Semiconductors*, Prentice-Hall Inc., New Jersey, 1971.
- [61] A.N. Banerjee, C.K. Ghosh, K.K. Chattopadhyay, *Sol. Energy Mater. Sol. Cells* 89 (2005) 75.
- [62] P. Kofstad, *Nonstoichiometry, Diffusion and Electrical Conductivity in Binary Metal Oxides*, Wiley-Interscience, Canada, 1972.
- [63] K. Koumoto, H. Koduka, W.S. Seo, *J. Mater. Chem.* 11 (2001) 251.